Carcinogenesis vol.35 no.8 pp.1881–1890, 2014
doi:10.1093/carcin/bgu121
Advance Access publication June 3, 2014

Nuclear adenomatous polyposis coli suppresses colitis-associated tumorigenesis in mice

Maged Zeineldin[1,2], Matthew A.Miller[1], Ruth Sullivan[3] and Kristi L.Neufeld[1,*]

[1]Department of Molecular Biosciences, University of Kansas, Lawrence, KS 66045, USA, [2]Department of Human Genetics, Medical Research Institute, Alexandria University, Alexandria, Egypt and [3]Carbone Cancer Center and Research Animal Resources Center, University of Wisconsin, Madison, WI 53706, USA

*To whom correspondence should be addressed. Department of Molecular Biosciences, University of Kansas, 7049 Haworth Hall, 1200 Sunnyside Avenue, Lawrence, KS 66045, USA. Tel: +1 785 864 5079; Fax: +1 785 864 5294; Email: klneuf@ku.edu

Mutation of tumor suppressor adenomatous polyposis coli (*APC*) initiates most colorectal cancers and chronic colitis increases risk. APC is a nucleo-cytoplasmic shuttling protein, best known for antagonizing Wnt signaling by forming a cytoplasmic complex that marks β-catenin for degradation. Using our unique mouse model with compromised nuclear Apc import (Apc^{mNLS}), we show that $Apc^{mNLS/mNLS}$ mice have increased susceptibility to tumorigenesis induced with azoxymethane (AOM) and dextran sodium sulfate (DSS). The AOM–DSS-induced colon adenoma histopathology, proliferation, apoptosis, stem cell number and *β-catenin* and *Kras* mutation spectra were similar in $Apc^{mNLS/mNLS}$ and $Apc^{+/+}$ mice. However, AOM–DSS-treated $Apc^{mNLS/mNLS}$ mice showed more weight loss, more lymphoid follicles and edema, and increased colon shortening than treated $Apc^{+/+}$ mice, indicating a colitis predisposition. To test this directly, we induced acute colitis with a 7 day DSS treatment followed by 5 days of recovery. Compared with $Apc^{+/+}$ mice, DSS-treated $Apc^{mNLS/mNLS}$ mice developed more severe colitis based on clinical grade and histopathology. $Apc^{mNLS/mNLS}$ mice also had higher lymphocytic infiltration and reduced expression of stem cell markers, suggesting an increased propensity for chronic inflammation. Moreover, colons from DSS-treated $Apc^{mNLS/mNLS}$ mice showed fewer goblet cells and reduced *Muc2* expression. Even in untreated $Apc^{mNLS/mNLS}$ mice, there were significantly fewer goblet cells in jejuna, and a modest decrease in colonocyte *Muc2* expression compared with $Apc^{+/+}$ mice. Colonocytes from untreated $Apc^{mNLS/mNLS}$ mice also showed increased expression of inflammatory mediators cyclooxygenase-2 (*Cox-2*) and macrophage inflammatory protein-2 (*MIP-2*). These findings reveal novel functions for nuclear Apc in goblet cell differentiation and protection against inflammation-induced colon tumorigenesis.

Introduction

As the second leading cause of cancer-related mortality in the USA, colorectal cancer (CRC) is responsible for nearly 50 000 deaths each year. Inflammation is considered a major risk factor for CRC and one in five persons with inflammatory bowel disease develop colon cancer. This colitis-associated cancer is characterized by poor prognosis and a relatively high mortality rate of ~50% (1). Anti-inflammatory drugs such as aspirin and celebrex can reduce the risk of CRC, not only in persons with inflammatory bowel disease but also in the general population (2). A better understanding of the contribution of inflammation to the underlying biology of CRC is needed to develop more effective preventive, diagnostic and therapeutic regimens.

Abbreviations: APC, adenomatous polyposis coli; AOM, azoxymethane; Cox, cyclooxygenase; CRC, colorectal cancer; CXCR-2, CXC cytokine receptor-2; DSS, dextran sodium sulfate; Gro-α, growth-related oncogene-α; IL, interleukin; MIP-2, macrophage inflammatory protein-2; mRNA, messenger RNA; NLS, nuclear localization signals; OPN, osteopontin; PBS, phosphate-buffered saline; TUNEL, terminal deoxynucleotidyl transferase dUTP nick end labeling.

Inflammation is a part of the immune response to harmful stimuli including pathogen invasion. However, extensive and/or prolonged inflammation can result in tissue damage. Tissue repair begins with the start of inflammation and both processes are controlled by several mediators and growth factors (3). Chronic inflammation and repair have been linked to tumor formation in several tissues (4).

The colonic mucosa has several lines of defense against the immunological challenges posed by foreign antigens and microorganisms to which it is continually exposed. Mucin produced by goblet cells coats the epithelial layer and provides a physical barrier against microbes (5). Other colon epithelial cells detect molecular structures that are associated with invading microbes (pathogen-associated molecular pattern) and secrete inflammatory mediators and anti-microbial compounds. In addition, tight junctions block passage of harmful molecules and pathogens between epithelial cells and into tissues. The colon also contains a collection of lymphoid tissues (gut-associated lymphoid tissues) and other immune cells that attack and destroy invading microbes. Collectively, these lines of defense are called the intestinal epithelial barrier (6). Disruption of this barrier is a hallmark of inflammatory bowel disease and inflammation-associated colon carcinogenesis (7). Experimentally, mice unable to produce mucus develop spontaneous inflammation and are at increased risk of colon tumor formation (8). In addition to the intestinal epithelial barrier, colonocytes are continuously generated from stem cells, replacing damaged cells at the luminal surface (9).

Adenomatous polyposis coli (*APC*) is the primary CRC suppressor gene, with *APC* mutations implicated in initiation of >80% of all CRC. The *APC* gene product is a large multidomain protein, which localizes to both the cytoplasm and nucleus (10). APC has many cellular functions, the most recognized being as a Wnt signaling pathway antagonist (11). In this capacity, APC forms a cytoplasmic complex with axin, glycogen synthase kinase 3β and other proteins that targets the oncoprotein β-catenin for proteasome-mediated degradation (12). APC also shuttles between the cytoplasm and the nucleus using at least two nuclear localization signals (NLS) and five nuclear export signals (13–15).

APC has several proposed nuclear functions. APC and β-catenin can interact in the nucleus leading to transcriptional repression of Wnt target genes and ultimately inhibition of cellular proliferation (12). Nuclear APC interacts with topoisomerase IIα, a critical enzyme required for DNA replication and a target for traditional cancer chemotherapeutics (16). Nuclear APC has also been implicated in DNA repair (17) and synthesis (18). Until recently, analyses of nuclear APC activities relied on purified proteins or cultured cells as there was no animal model to enable characterization of nuclear APC functions in the context of a whole organism.

To better understand the role of nuclear APC in tissue homeostasis and tumor suppression, we generated a mouse model in which the nuclear import of Apc was compromised by the introduction of mutations into each NLS (19). We found that these mutant mice ($Apc^{mNLS/mNLS}$) have higher rates of cellular proliferation than their wild-type counterparts and increased expression of Wnt target genes (19). We also found that $Apc^{Min/+}$ mice, the most widely utilized mouse model of intestinal polyposis mediated by truncating germline *Apc* mutation, develop more and larger intestinal polyps when they also harbor the Apc^{mNLS} allele ($Apc^{mNLS/Min}$). Together these data suggest a tumor suppressor function for nuclear Apc (19).

In this study, we tested the potential roles for nuclear Apc in a mouse model of colitis-mediated colon cancer. In this model, colon cancers are initiated with a single injection of the mutagen, azoxymethane (AOM) and are promoted with repeated oral administration of dextran sodium sulfate (DSS) to induce colonic inflammation (20). Using this model, we examined the requirement of nuclear APC in suppression of colitis-associated CRC. In contrast with the polyps that

predominantly develop in the small intestines of $Apc^{Min/+}$ mice (21,22), the AOM–DSS-treated mice develop tumors in the colon, the site of tumor formation in humans with mutated *APC* (23). Furthermore, most mouse models with germline *Apc* mutations express truncated Apc lacking both β-catenin degradation and nuclear localization domains (22). *Apc* mutations are not typically found in colon tumors from AOM–DSS-treated mice. Rather, mutations in β-catenin that render it incapable of Apc-mediated destruction are considered the initiating step (20). This feature allows us to distinguish tumor suppressor functions of nuclear Apc from the cytoplasmic role of Apc in targeting β-catenin for destruction.

Here, we show that nuclear Apc suppresses colon tumorigenesis in the AOM–DSS mouse model. Although they differ in relative number, the colonic polyps themselves show very similar histology, β-catenin mutations, apoptosis, stem cell number and proliferation indices in AOM–DSS-treated $Apc^{mNLS/mNLS}$ and $Apc^{+/+}$ mice. $Apc^{mNLS/mNLS}$ mice are also more sensitive to DSS-induced colitis with fewer stem cells and proportionally less crypt branching relative to ulceration extent, suggesting less ability to repair inflammation-induced tissue damage. These mice also display a goblet cell deficiency, consistent with a role for nuclear Apc in goblet cell differentiation. Based on the cumulative data obtained using the Apc^{mNLS} model, we propose that nuclear Apc protects against colitis-associated colon tumorigenesis by suppressing inflammation, inhibiting Wnt signaling, and increasing colonocyte differentiation and mucus production.

Materials and methods

Mouse husbandry

Mice were maintained at the animal care unit at the University of Kansas according to animal use statement number 137-01. The research complied with all relevant federal guidelines and institutional policies. Mice were fed *ad libitum* with Purina Lab Diet 5001 and were housed in cages in adjoining animal rooms. All mice are C57BL/6J and $Apc^{mNLS/mNLS}$ mice are congenic (>N15).

Acute inflammation model and colitis severity clinical scoring

Thirteen $Apc^{mNLS/mNLS}$ and 14 $Apc^{+/+}$ mice (6–7-week-old) were provided 2.5% DSS (MW 36 000–50 000, MP Cat# 160110) in their drinking water for 7 days followed by 5 days with regular water. DSS used in both test and control groups was from the same batch. Animal weight, stool consistency and presence or absence of blood in stool were recorded daily. At study's end, mice were killed and colons removed from cecum to anus and opened longitudinally. Pictures were taken of opened and intact colon. Clinical scoring of colitis severity was performed as described previously (24), briefly; 0 = normal, 1 = few formed pellets to semi-solid stool, 2 = semi-solid to fluid stool with or without definite evidence of blood, 3 = bloody stool, 4 = bloody fluid and 5 = no content. A small (1 mm diameter) piece of tissue was snap-frozen in liquid nitrogen in 1 ml Trizol® and stored at −80°C for RNA preparation according to manufacturer instructions and complementary DNA was prepared as described previously (19).

Scoring goblet cells in the small intestine and colons

Intestinal pieces were fixed overnight in formalin as Swiss-rolls then stored in 70% ethanol until they were paraffin embedded. Sections (6 µm) were stained with Alcian Blue to visualize goblet cells and counter stained with Neutral red or hematoxylin. Goblet cells were assessed in 439 crypts from jejuna and 409 crypts from ilea of four $Apc^{mNLS/mNLS}$ mice and in 383 crypts from jejuna and 327 crypts from ilea of three $Apc^{+/+}$ mice. Goblet cells were scored as the percentage of the total cells per crypt by an investigator who was blind to the genotypes.

Analysis of messenger RNA from colon epithelial cells by real-time reverse transcription–PCR

Epithelial cells from $Apc^{mNLS/mNLS}$ and $Apc^{+/+}$ mice were isolated from whole colons as described previously (19,25). Briefly, colons were removed, washed in phosphate-buffered saline (PBS) and incubated in 0.04% sodium hypochlorite. After washing in PBS, colons were incubated in solution B (2.7 mM KCl, 150 mM NaCl, 1.2 mM KH_2PO_4, 680 mM Na_2HPO_4, 1.5 mM ethylenediaminetetraacetic acid and 0.5 mM dithiothreitol) on ice. Every 15 min, colons were transferred into new tubes with PBS and vortexed for 15 s and then incubated in solution B. The process of incubation and vortex was repeated twice to collect epithelial cells following centrifugation for 5 min at 4°C. Cells were washed twice in PBS, collected following centrifugation and finally suspended in 1 ml of PBS. RNA extraction, complementary DNA formation and quantitative-PCR using gene-specific primers (listed in Table I) were performed as described previously (19).

AOM–DSS treatment

Fifteen $Apc^{mNLS/mNLS}$ and 8 $Apc^{+/+}$ mice (6-week-old) received an intra-peritoneal injection of 7.5 mg/kg AOM followed by three cycles, 5 days each, of 2.5% DSS in their drinking water at 7, 10 and 13 weeks. Fourteen $Apc^{mNLS/mNLS}$ and 10 $Apc^{+/+}$ mice were not treated and served as control groups. DSS used in both test and control groups was from the same batch. Mice were killed at 24 weeks, then the large intestine from the cecum to the anus was processed as described previously for the acute inflammation study. Colonic polyps and lymphoid follicles were identified and measured by an investigator blind to the animal's genotype using a dissecting microscope with 10 magnification and with the aid of an eyepiece graticule calibrated to a 50 mm scale stage micrometer with 0.1 and 0.01 mm graduation (Leica).

Histopathological examination and scoring

Tumors and representative lymphoid follicles were dissected from the surrounding tissues, processed and paraffin embedded. Colons from the cecum to the anus were Swiss-rolled, paraffin embedded, sectioned (8 µm) and stained with hematoxylin and eosin for histopathological analysis. Colon tissue from the acute inflammation study was scored using a modified system from that described by Cooper *et al.* (26) and summarized in Supplementary Methods, available at *Carcinogenesis* Online.

Detection of Ctnn1b (b-catenin) and Kras mutations

DNA was extracted using the QIAamp DNA formalin-fixed paraffin-embedded tissue kit (Qiagen) from 3–8 manually microdissected, 8 µm sections of paraffin-embedded tissue for each tumor and amplified using primers spanning b-catenin (*Ctnn1b*) exon 3 (forward: 5′-TTCAGGTAGCATTTTCAGTTCA-3′; reverse: 5′-TGCTAGCTTCCAAACACAAATGC-3′) and *Kras* exon 1 (forward: 5′-TGTAAGGCCTGCTGAAAATG-3′; reverse: 5′-GCACGCAGACTGTAG AGCAG-3′). Gel-purified PCR products were sequenced (ACGT Inc.).

Assessment of proliferation

Paraffin-embedded tumors were sectioned (8 µm) and stained for proliferation marker Ki-67 as described previously (19). Images from at least three fields per tumor (100 × 100 µm) were analyzed for Ki-67-positive cells at ×40 magnification.

Assessment of apoptosis

Apoptosis was detected using a terminal deoxynucleotidyl transferase dUTP nick end labeling (TUNEL) assay DeadEnd™ Fluorometric TUNEL System

Table I. Primers to quantify inflammatory mediators shown previously to be differentially expressed in $Apc^{Min/+}$ polyps and stem cell markers

Gene	Forward primer	Reverse primer
Cox-1	5′-AAGGAGTCTCTCGCTCTGG-3′	5′-CTGGTTCTGGCACGGATAGT-3′
Cox-2	5′-CATTCTTTGCCCAGCACTTC-3′	5′-GGCGCAGTTTATGTTGTCTG-3′
CXCR-2	5′-AGCAGAGGATGGCCTAGTCA-3′	5′-TCCACCTACTCCCATTCCTG-3′
Gro-α	5′-TGTTGTGCGAAAAGAAGTGC-3′	5′-TACAAACACAGCCCTCCCACA-3′
MIP-2	5′-CAGACTCCAGCCACACTTCA-3′	5′-CAGTTCACTGGCCACAACAG-3′
Opn	5′-GCTTGGCTTATGGACTGAGG-3′	5′-GACTCACCGCTCTTCATGTG-3′
Muc2	5′-GGAATTTGCTGTGCACCTGA-3′	5′-GCTGTAGTGTGGGGTGCTGA-3′
Bmi1	5′-CAGAAATCGATCGAACAACAA-3′	5′-GGACAATACTTGCTGGTCTCC-3′
Hopx	5′-GGTCTCACGGAGCAGAC-3′	5′-AAGCCGAGGGAAGGAAGAAG-3′
HGPRT	5′-TGCTCGAGATGTCATGAAGG-3′	5′-TATGTCCCCCGTTGACTGAT-3′

(Promega) following manufacturer's instructions. The number of positive cells in 4–5 fields (× 40 magnifications) per tumor was determined.

Stem cell scoring

Formalin-fixed paraffin-embedded tissues were sectioned (7 µm), deparaffinized in SafeClear (Fisher Scientific) and rehydrated in ethanol. Antigen retrieval was performed by boiling the slides in 10 mM citrate buffer (pH 6.0) for 25 min in a microwave. Anti-DCAMKL1 antibody (1:100, ab31704; Abcam) was used for primary staining with Alexafluor goat anti-rabbit 564 (Molecular Probes) as a secondary and 4′,6-diamidino-2-phenylindole as a nuclear stain. Positive cells in whole Swiss-rolled colon sections were counted by an investigator blind to the genotype.

Statistical analysis

P-values were calculated using Student's *t*-test, Mann–Whitney non-parametric tests, Fisher's exact test and *GraphPad Prism* software as indicated in figure legends. The distribution of exon 3 mutations in AOM/DSS-treated $Apc^{mNLS/mNLS}$ and $Apc^{+/+}$ mice was analyzed using a one-way analysis of variance. Statistical analysis of goblet cell scores in small intestines from untreated mice was performed by Dr J.Wick, Department of Biostatistics at The University of Kansas Medical Center. A linear mixed model was used as described previously (27). The mixed model approach utilizes an analysis of variance model with an additional random 'mouse' effect to model the inherent correlation that exists between samples from the same mouse. We assumed the random mouse effect is normally distributed with zero mean and unknown variance.

Results

$Apc^{mNLS/mNLS}$ mice have increased susceptibility to colitis-associated tumorigenesis

We previously reported that the Apc^{mNLS} allele increases intestinal tumorigenicity in mice harboring a germline mutation that results in Apc truncation, Apc^{Min} (19). In both $Apc^{Min/+}$ and $Apc^{mNLS/Min}$ mice, the vast majority of tumors develop in the small intestine (19). To examine the role of nuclear Apc as a suppressor of colon cancer, we initiated colon tumors with the mutagen AOM followed by cycles of DSS to induce chronic inflammation (Figure 1A). Unlike tumors in $Apc^{Min/+}$ mice, AOM–DSS-treated wild-type mice develop colonic tumors, which do not typically have *Apc* mutations (20).

Of the 15 $Apc^{mNLS/mNLS}$ mice, five (33%) developed rectal prolapse and were killed at age 20.6, 20.6, 21, 21 and 22.6 weeks, whereas only one of the eight treated $Apc^{+/+}$ mice required early termination (at 22.9 weeks) due to rectal bleeding. The remaining mice were killed at 24 weeks. Two untreated control groups of 14 $Apc^{mNLS/mNLS}$ and 10 $Apc^{+/+}$ mice were also killed at 24 weeks of age, at which time none displayed detectable colon polyps. There were no detectable tumors in the small intestines from AOM–DSS-treated $Apc^{mNLS/mNLS}$ and $Apc^{+/+}$ mice (data not shown). However, while all of the AOM–DSS-treated $Apc^{mNLS/mNLS}$ mice developed at least one colonic polyp, over one-third of the treated $Apc^{+/+}$ mice remained free of colon tumors at the end of the study (Figure 1B–D). Moreover, in AOM–DSS-treated $Apc^{mNLS/mNLS}$ mice, colonic polyp numbers were more than double that of treated $Apc^{+/+}$ mice (Figure 1E). Based on these results, we conclude that AOM–DSS-treated $Apc^{mNLS/mNLS}$ mice have higher tumor incidence and multiplicity than treated $Apc^{+/+}$ mice.

To determine the mechanism by which Apc^{mNLS} increases polyp formation in the AOM–DSS model, we investigated several predicted contributory elements. Histopathological examination of 20 polyps from AOM–DSS-treated $Apc^{mNLS/mNLS}$ mice and 10 tumors from treated $Apc^{+/+}$ mice indicated that all were polypoidal, semi-flat or flat adenomas with some degree of atypia (Figure 1F and G). Moderate to marked lymphoplasmacytic infiltration was observed in most polyps with varying degree of inflammatory reactions. Polyp size in treated $Apc^{mNLS/mNLS}$ and $Apc^{+/+}$ mice did not significantly differ between groups (Figure 2A). There was also no significant difference in proliferation level as assessed by proliferation marker, Ki-67 (Figure 2B and C) nor in apoptosis as detected by TUNEL assay (Figure 2D and E). Staining for the intestinal stem cell marker DCAMKL1, we found only a few positive cells, mainly at the tumor base, with no significant difference between tumors from both groups (data not shown). Taken together, it appears that adenoma growth is not altered in AOM–DSS-treated $Apc^{mNLS/mNLS}$ mice.

Stabilizing mutations in *Ctnn1b* (b-catenin) exon 3 are characteristic of tumors from mice treated with AOM–DSS, with activating mutations in *Kras* codon 1 found later in development. We identified mutations in β-catenin exon 3 in each of the nine examined adenomas from AOM–DSS $Apc^{+/+}$ mice and in 24 of 25 examined adenomas from treated $Apc^{mNLS/mNLS}$ mice (Figure 2F–H). Furthermore, the specific missense mutations in *Ctnn1b* (b-catenin) were similar in both groups (Figure 2G and H, $P = 0.22$). No mutations were found in exon 1 of *kras* in tumors from either group, indicating that the tumors were at an early stage of progression (data not shown).

Weight loss and shortening of colon length are considered inflammation parameters in AOM–DSS mouse models (23). We found that AOM–DSS-treated $Apc^{mNLS/mNLS}$ mice lost significantly more weight than treated $Apc^{+/+}$ mice relative to the corresponding untreated control groups (Figure 2I). Colon lengths were reduced by 12% in treated $Apc^{mNLS/mNLS}$ mice and by only 8% in treated $Apc^{+/+}$ mice (Figure 2J). Untreated $Apc^{mNLS/mNLS}$ and $Apc^{+/+}$ mice had similar numbers of colonic lymphoid follicles visible with the aid of a dissecting microscope with ×10 magnification (Figure 2K) and there were no significant differences in the number of small intestinal lymphoid follicles in AOM–DSS-treated $Apc^{mNLS/mNLS}$ and $Apc^{+/+}$ mice (data not shown). However, the AOM–DSS-treated $Apc^{mNLS/mNLS}$ mice had significantly more visible colonic lymphoid follicles than the treated $Apc^{+/+}$ mice (Figure 2K). Furthermore, three of the five AOM–DSS-treated $Apc^{mNLS/mNLS}$ mice analyzed showed residual mild mucosal edema, whereas only one of five treated $Apc^{+/+}$ mice analyzed displayed histopathological signs of edema (data not shown). Together, these data are indicative of more severe inflammation in colons of AOM–DSS-treated $Apc^{mNLS/mNLS}$ mice than in treated $Apc^{+/+}$ mice.

$Apc^{mNLS/mNLS}$ mice are more susceptible to DSS-induced colitis

To more directly examine the role of nuclear Apc in inflammation, $Apc^{mNLS/mNLS}$ mice were provided 2.5% DSS in their drinking water for 7 days to induce acute inflammation and then analyzed after five additional days of recovery. Starting at day 7, DSS-treated $Apc^{mNLS/mNLS}$ mice lost significantly more weight than treated $Apc^{+/+}$ mice (Figure 3A). Once returned to regular water, DSS-treated $Apc^{+/+}$ mice showed first signs of weight gain one day prior to treated $Apc^{mNLS/mNLS}$ mice (days 10 and 11, respectively), indicating delayed recovery in the DSS-treated $Apc^{mNLS/mNLS}$ mice. At the end of the 12 day study, DSS-treated $Apc^{mNLS/mNLS}$ mice showed clinical signs indicating more severe colitis than treated $Apc^{+/+}$ mice (Figure 3B). Histopathological assessment of colon tissue revealed more extensive ulceration and more severe inflammation in DSS-treated $Apc^{mNLS/mNLS}$ mice compared with treated $Apc^{+/+}$ mice (Figure 3K–N). Scoring the extent of ulceration and inflammation confirmed that these differences were significant (Figure 3C and D).

Tissue inflammation and regeneration are physiologically linked processes aimed at dealing with injury and repairing the damage (3). One key component of regeneration is the ability of stem cells to repopulate damaged tissues. Intestinal stem cell markers *Hopx* and *Bmi1* messenger RNA (mRNA) were significantly reduced in colons from DSS-treated $Apc^{mNLS/mNLS}$ mice relative to those from treated $Apc^{+/+}$ mice (Figure 3E and F). We also found significant reduction in the number of cells expressing the intestinal stem cell marker DCAMKL1 in colons from DSS-treated $Apc^{mNLS/mNLS}$ mice compared with those from $Apc^{+/+}$ mice (Figure 3H–J). Collectively, these data indicate stem cell deficiency in the DSS-treated $Apc^{mNLS/mNLS}$ mouse colon. The expression of *Bmi1* and *Hopx* and the number of DCAMKL1-positive cells did not significantly differ in colons from untreated $Apc^{mNLS/mNLS}$ and $Apc^{+/+}$ mice (data not shown).

Intestinal crypts can increase in number by crypt branching and fission (28,29). In DSS-treated $Apc^{+/+}$ mice, there was a strong positive correlation between ulceration and crypt branching, whereas in treated $Apc^{mNLS/mNLS}$ mice, this correlation was not seen (Figure 3G). Other parameters for modified colonic epithelial architecture including crypt separation, crypt shortening and enlarged and elongated

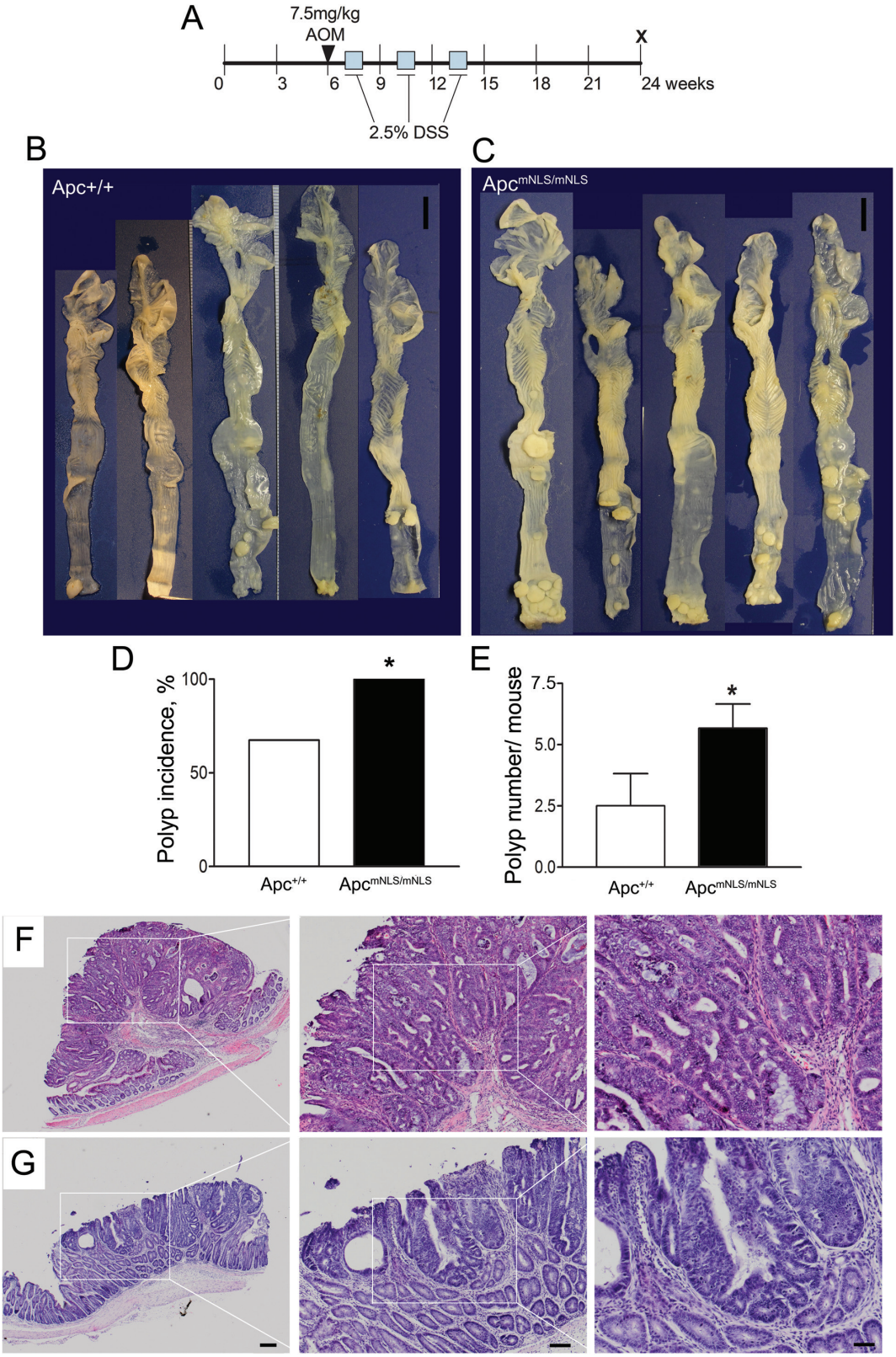

Fig. 1. Apc^{mNLS} allele increases tumor incidence and multiplicity in AOM–DSS mouse model. AOM–DSS treatment protocol (**A**). Representative samples of large intestines from treated Apc$^{+/+}$ (n = 8) mice (**B**) and Apc$^{mNLS/mNLS}$ (n = 15) mice (**C**). Scale bars = 1 cm. (**D**) Polyp incidence calculated following polyp detected using a dissecting microscope with ×10 magnification. Significant differences are indicated with * ($P < 0.05$, Fisher's exact test). (**E**) Average polyp number in AOM-DSS treated mice ($P < 0.05$, Student's t-test). Histopathology of representative polypoidal (**F**) and semi-flat (**G**) colonic adenomas from AOM–DSS-treated Apc$^{mNLS/mNLS}$ mice. Higher magnifications of boxed areas are presented. Scale bars 200 µm (left panels), 100 µm (middle) and 50 µm (right). Error bars represent standard error of the mean throughout.

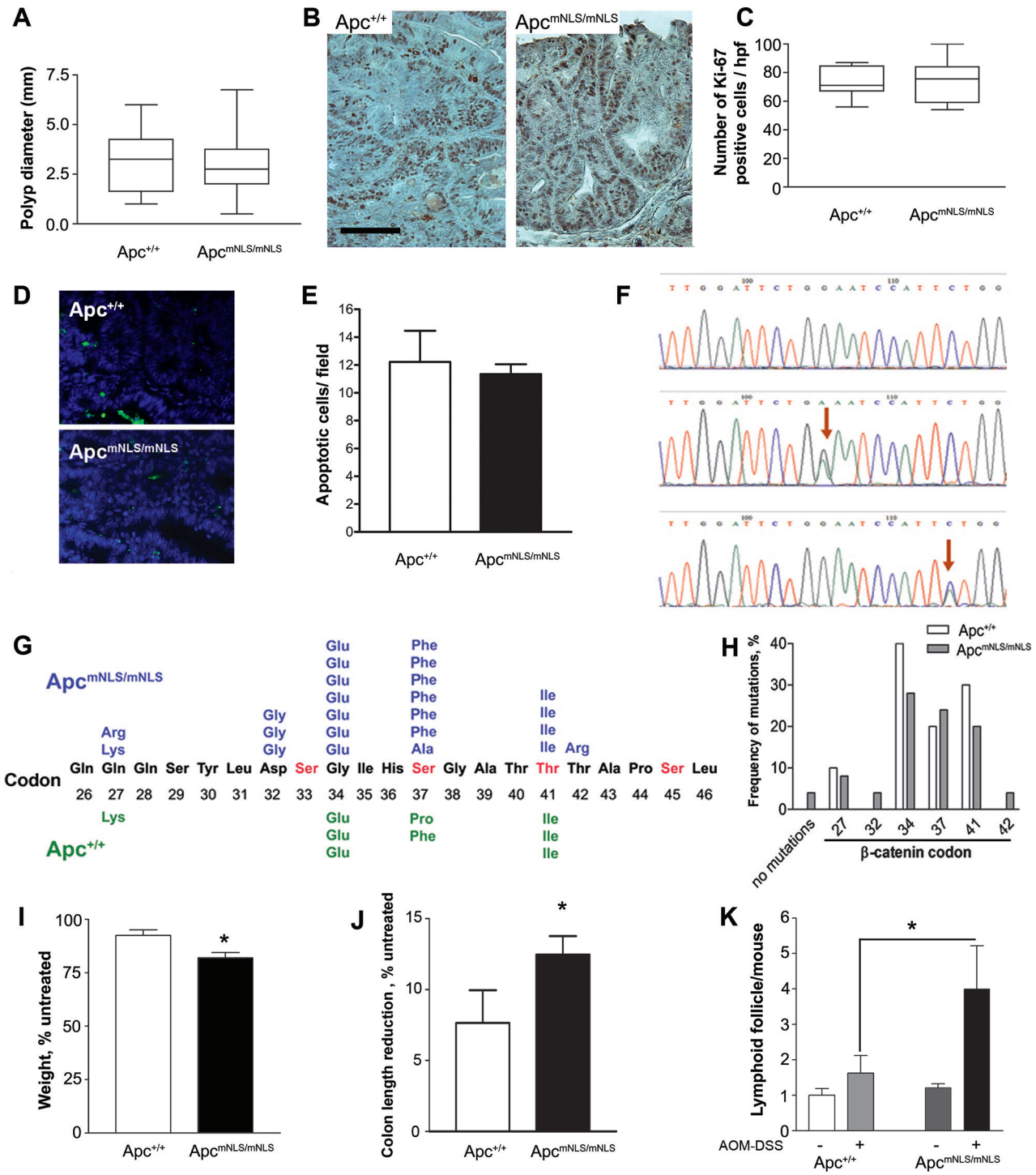

Fig. 2. Polyps from AOM–DSS-treated Apc$^{mNLS/mNLS}$ mice do not differ in size, proliferation, apoptosis or β-catenin mutations, but treated Apc$^{mNLS/mNLS}$ mice are more prone to chronic inflammation. (**A**) Colon polyp diameters from AOM–DSS-treated Apc$^{mNLS/mNLS}$ and Apc$^{+/+}$ mice presented as box and whiskers plots. (**B**) Representative images of Ki-67 staining, scale bar = 100 μm. (**C**) Box and whiskers plots of proliferation marker Ki-67-positive cells per 100 × 100 μm high-power field (hpf) from AOM–DSS-treated Apc$^{mNLS/mNLS}$ and Apc$^{+/+}$ mice. (**D**) Representative images of TUNEL assay showing apoptotic cells in green and 4′,6-diamidino-2-phenylindole (DAPI)-stained nuclei in blue. (**E**) The average number of apoptotic cells per high-power field (×40) in tumors from AOM–DSS-treated Apc$^{+/+}$ (upper panel) and Apc$^{mNLS/mNLS}$ (lower panel) mice. (**F**) Representative sequencing chromatographs showing a G→A (middle) or a C→T (lower) mutation (arrows) or the normal control β-catenin coding sequence (top). (**G**) Predicted amino acid alterations resulting from the missense mutations in exon 3 of β-catenin are presented for polyps from AOM–DSS-treated Apc$^{mNLS/mNLS}$ (top) and Apc$^{+/+}$ (bottom) mice. (**H**) The distribution of β-catenin exon 3 mutations found in tumors from Apc$^{mNLS/mNLS}$ and Apc$^{+/+}$ mice is displayed as the relative frequency at each codon. (**I**) The average weight change of AOM–DSS-treated mice is shown relative to the untreated mice from both Apc$^{mNLS/mNLS}$ and Apc$^{+/+}$ groups (*$P < 0.01$, Student's *t*-test). (**J**) The average reduction of colon length in AOM–DSS-treated mice as a percentage to the untreated mice (*$P < 0.05$, Student's *t*-test). (**K**) The average number of visible colonic lymphoid follicles in untreated and AOM–DSS-treated mice (*$P < 0.05$, Student's *t*-test). Error bars represent standard error of the mean throughout.

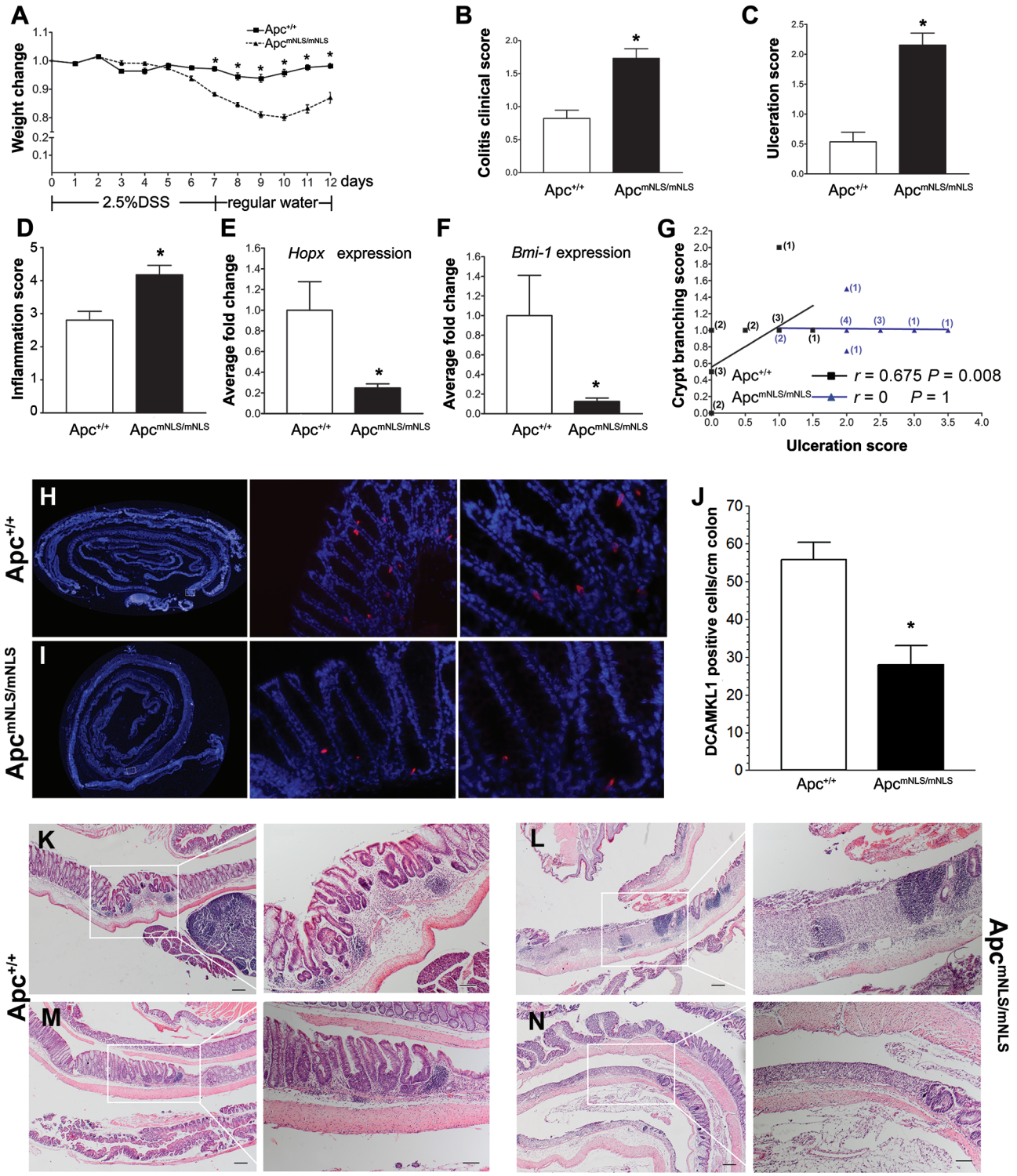

Fig. 3. DSS induces more severe tissue damage and less effective tissue repair in Apc$^{mNLS/mNLS}$ mice. (**A**) Weight changes in 2.5% DSS-treated Apc$^{mNLS/mNLS}$ and Apc$^{+/+}$ mice (treatment schematic shown below graph). * indicates $P < 0.05$, using Student's *t*-test. (**B**) The average colitis severity clinical score in DSS-treated Apc$^{mNLS/mNLS}$ and Apc$^{+/+}$ mice ($P < 0.05$, using Mann–Whitney test). (**C** and **D**) Histopathological scoring for ulceration (C) and inflammation (D) in DSS-treated Apc$^{mNLS/mNLS}$ and Apc$^{+/+}$ mice ($P < 0.05$, using Mann–Whitney test). (**E** and **F**) Relative expression of the intestinal stem cell markers; *Hopx* (E) and *Bmi1* (F) in DSS-treated Apc$^{+/+}$ and Apc$^{mNLS/mNLS}$ mice ($P < 0.05$, using Mann–Whitney test). (**G**) Correlation between ulceration score and crypt branching score in 14 DSS-treated Apc$^{+/+}$ (black squares) and 13 treated Apc$^{mNLS/mNLS}$ mice (blue triangles). The number of mice at each point are presented in black (Apc$^{+/+}$) and blue (Apc$^{mNLS/mNLS}$). (**H**–**J**) Intestinal stem cell marker DCAMKL (red) in colons from DSS-treated Apc$^{+/+}$ (H) and Apc$^{mNLS/mNLS}$ (I) mice. The average number of positive cells/cm of colon from DSS-treated mice is presented in (J) ($P < 0.05$, Student's *t*-test). (**K**–**N**) Representative pictures of colonic lesions from DSS-treated Apc$^{+/+}$ mice (K and M) and treated Apc$^{mNLS/mNLS}$ mice (L and N) showing inflammation with no ulceration and lymphocytic infiltration (K), ulceration with lymphocytic infiltrations (L), crypt branching (M) and ulceration (N). Scale bars 200 µm (left panels) and 100 µm (right panels).

crypts did not show significant differences between colons from DSS-treated $Apc^{+/+}$ and treated $Apc^{mNLS/mNLS}$ mice (data not shown). Tumors were not seen in any of the acutely DSS-treated mice and only one mouse exhibited epithelial dysplasia that was not associated with inflammation. Together, these data suggest that regeneration in DSS-treated $Apc^{mNLS/mNLS}$ mice is lagging that of treated $Apc^{+/+}$ mice and that $Apc^{mNLS/mNLS}$ mice are more susceptible to DSS-induced acute inflammation than their wild-type counterparts.

$Apc^{mNLS/mNLS}$ mice have fewer goblet cells

While examining hematoxylin- and eosin-stained tissue from DSS-treated mice, we found that colons from treated $Apc^{mNLS/mNLS}$ mice appeared to have fewer goblet cells than those from treated $Apc^{+/+}$ mice. This observation was confirmed using Alcian Blue, which stains mucopolysaccharides and thus marks goblet cells. Colons from DSS-treated $Apc^{mNLS/mNLS}$ mice had fewer and lighter-staining goblet cells than those from DSS-treated $Apc^{+/+}$ mice (Figure 4A–D). Moreover, a significantly lower level of *Muc2* mRNA (the major colonic mucin) was found in colon epithelia from DSS-treated $Apc^{mNLS/mNLS}$ mice than in treated $Apc^{+/+}$ mice, further validating the goblet cell phenotype originally noted in colon tissue sections (Figure 4E).

Goblet cells secrete mucus that serves as a protective barrier from microbes and foreign antigens, which could otherwise induce inflammation (5). Reduction of goblet cell number is associated with both ulcerative colitis and colorectal carcinoma; Apc and reduced Wnt signaling have been implicated in goblet cell differentiation (30). Therefore, we predicted that alterations in goblet cell abundance might even be detected in tissue from untreated $Apc^{mNLS/mNLS}$ mice, which showed elevated expression of Wnt targets (19). There were significantly fewer goblet cells in jejuna from untreated $Apc^{mNLS/mNLS}$ mice than in $Apc^{+/+}$ mice (Figure 4G). Although not statistically significant, the same trend was also seen in the ileum (data not shown). Colon crypts from untreated mice contain such a high proportion of goblet cells that their accurate quantification is challenging. Using *Muc2* mRNA levels as an indirect assessment of goblet cell abundance, we found a reduction in *Muc2* mRNA in colonocytes from untreated $Apc^{mNLS/mNLS}$ mice compared with those from untreated $Apc^{+/+}$ mice, albeit not of statistical significance (Figure 4F, $P = 0.073$). We conclude that $Apc^{mNLS/mNLS}$ mice have fewer goblet cells than $Apc^{+/+}$ mice.

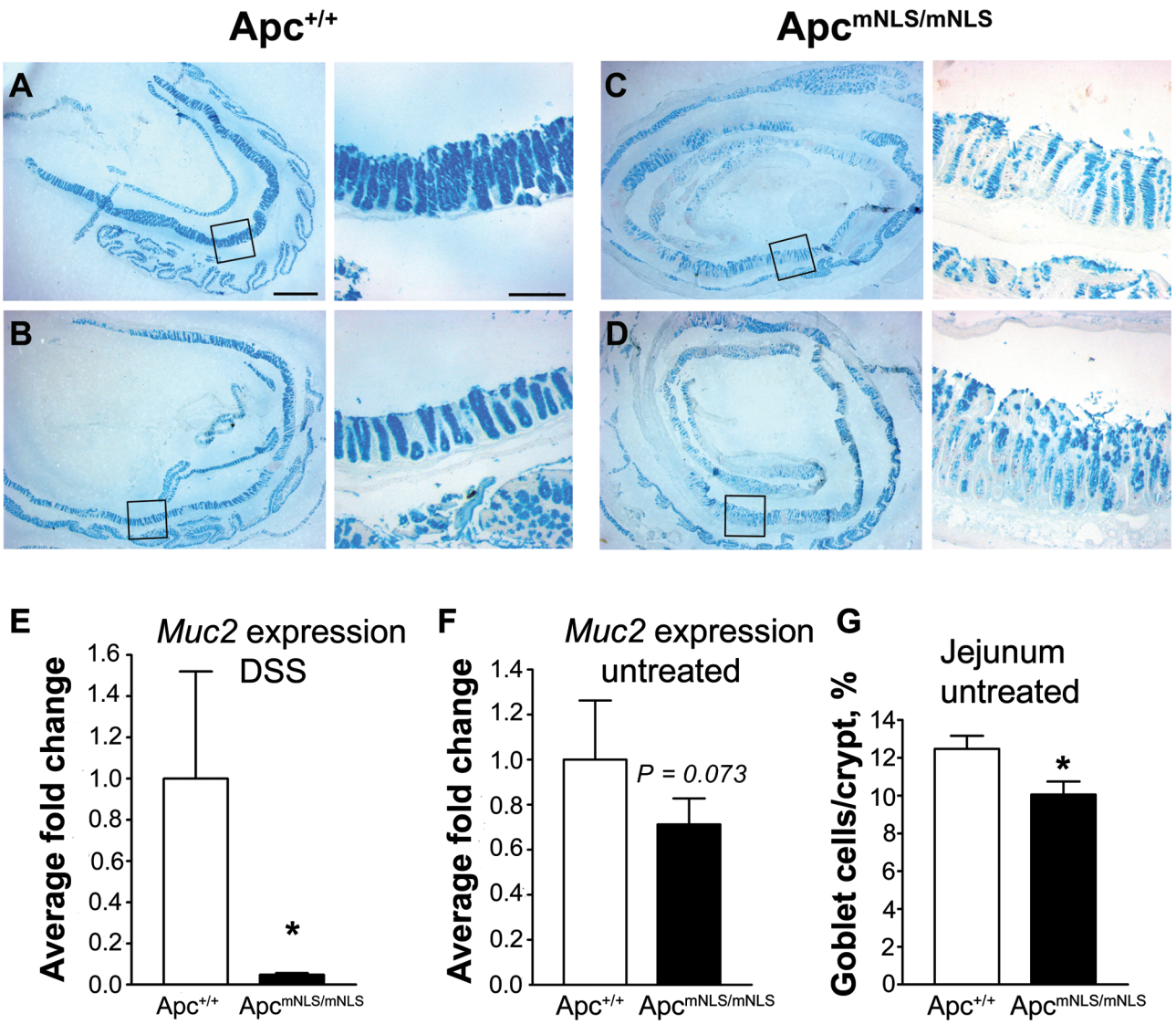

Fig. 4. $Apc^{mNLS/mNLS}$ mice have goblet cell defects. (**A**–**D**) Alcian Blue-stained sections of colons in DSS-treated $Apc^{+/+}$ (A and B) and $Apc^{mNLS/mNLS}$ mice (C and D). Left panels show the whole Swiss roll. The squared areas in the left panels are magnified in right panels. (**E** and **F**) Relative expression of *Muc2* mRNA in DSS-treated (E) and untreated (F) $Apc^{+/+}$ and $Apc^{mNLS/mNLS}$ mice (*$P < 0.05$, using Mann–Whitney test). (**G**) Goblet cells represented as percentage of total cells per crypt in jejunum from untreated $Apc^{+/+}$ and $Apc^{mNLS/mNLS}$ mice (*$P < 0.05$, using mixed statistical model as described in Materials and methods). Error bars throughout represent standard error of the mean.

Increased expression of inflammatory mediators in colon epithelial cells from untreated Apc$^{mNLS/mNLS}$ mice

Early genetic changes in colon tumorigenesis have recently been implicated in altered mucus production and inflammatory response (31). To more directly connect the goblet cell reduction in Apc$^{mNLS/mNLS}$ mice with inflammation, we quantified mRNA of presumed inflammatory mediators in colonic epithelial cells isolated from untreated Apc$^{mNLS/mNLS}$ mice and untreated Apc$^{+/+}$ control mice. We analyzed inflammation-associated genes that were reported to be differentially expressed in colon adenomas that develop in Apc$^{Min/+}$ mice (32): *osteopontin (OPN), macrophage inflammatory protein-2 (MIP-2), growth-related oncogene-α (Gro-α), CXC cytokine receptor-2 (CXCR-2),* and *cyclooxygenase-1* and *-2 (Cox-1 and Cox-2)*. There were no significant differences in the expression levels of *Cox-1*, *CXCR-2, Gro-α* and *Opn* in Apc$^{mNLS/mNLS}$ samples relative to Apc$^{+/+}$samples (data not shown). However, *Cox-2* and *MIP-2* mRNA levels were each significantly higher in colonocytes from untreated Apc$^{mNLS/mNLS}$ mice compared with those from Apc$^{+/+}$ mice (Figure 5). The finding that both *Cox-2* and *MIP-2* are upregulated in colonocytes from untreated Apc$^{mNLS/mNLS}$ mice supports a role for nuclear Apc in suppressing colitis.

Discussion

Promiscuous Wnt signaling is a hallmark of CRC in both sporadic and colitis-associated cases, but this promiscuity is the result of different genetic events. Although *APC* mutation is the initiating event in most sporadic cases, APC-independent β-catenin activation is often an early event in colitis-associated CRC. In the latter case, mutation of *APC* still occurs, however at a later stage of tumor formation (1). This tendency is recapitulated in a mouse model of colitis-associated CRC, in which a single dose injection of the mutagen AOM leads to 'stabilizing' mutations in β-catenin, followed by cycles of DSS to induce colon inflammation (20). A single dose of AOM without subsequent DSS treatment results in only a very low tumor incidence (33), emphasizing that aberrant regulation of Wnt signaling by β-catenin stabilization is not sufficient for tumor formation and inflammation is also required. In contrast, truncation of APC can initiate tumor formation in both humans and rodent models. Furthermore, most human colon cancers display *APC* mutations, whereas tumors in other organs often show mutations in other Wnt pathway components, indicating a Wnt-independent, colon-specific, tumor suppressor function of APC (11). Together, this evidence supports two distinct tumor suppressor roles for APC that must be eliminated during CRC progression: Wnt signaling regulation and inflammation suppression. Mutations of *APC* early in sporadic cases of CRC might suffice to fulfill both requirements of Wnt signaling activation and induction of inflammation as seen in colitis-associated CRC.

Data supporting a role for APC/Apc in suppressing colitis already exist (31,34). Many inflammatory mediators are upregulated in Apc$^{Min/+}$ polyps including Cox-1, Cox-2, MIP-2, OPN, CXCR-2 and Gro-α (32). Although Cox-2 is generally considered a Wnt target (35–37), the other genes are not. Moreover, inflammatory cytokines, interleukin (IL)-23 and IL-17, were elevated in polyps from human CRC and in colons from mice with a conditional Apc mutation (31). Furthermore, reducing inflammation decreases tumor incidence in both humans and mouse models with germline *APC* mutations (2,38).

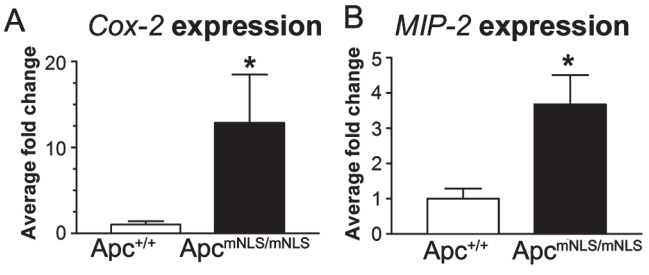

Fig. 5. Differential expression of inflammatory mediators in untreated Apc$^{mNLS/mNLS}$ mice. Relative expression of *Cox-2* and *MIP-2* in colon epithelial cells from untreated Apc$^{mNLS/mNLS}$ and Apc$^{+/+}$ mice (*$P < 0.05$ using Mann–Whitney non-parametric test). Error bars represent standard error of the mean.

Here, we report that Apc$^{mNLS/mNLS}$ mice have increased colitis-associated tumor susceptibility as indicated by an increase in both polyp incidence and multiplicity after treatment with AOM–DSS (Figure 1). We found no change in polyp size, apoptosis or cell proliferation in the polyps from AOM–DSS-treated Apc$^{mNLS/mNLS}$ mice. In addition, there was no difference in histopathology or in the number of stem cells in polyps from AOM–DSS-treated Apc$^{+/+}$ and Apc$^{mNLS/mNLS}$ mice and they possessed the same spectrum of exon 3 *Ctnn1b* (b-catenin) mutations and no *Kras* mutations (Figure 2). Together, these findings suggest loss of nuclear Apc does not change molecular and morphological characteristics of colitis-induced colon tumors. One possible explanation for these finding is that reduction in nuclear Apc enhances colitis. In support of this idea, we found that Apc$^{mNLS/mNLS}$ mice have higher susceptibility to DSS-induced colitis (Figure 3) with a greater tendency to progress into chronic inflammation (Figures 2 and 3). This progression was manifested by weight loss, increased ulceration and inflammation score, and more lymphocytic infiltration and lymphoid nodules in colons from DSS-treated Apc$^{mNLS/mNLS}$ mice relative to those from treated Apc$^{+/+}$ controls. Of note, we detected signs of inflammation as shown by upregulation of the inflammatory mediators *Cox-2* and *MIP-2* even in untreated Apc$^{mNLS/mNLS}$ mice. As inflammation is a major risk factor for CRC, our findings support another tumor suppressor role of Apc to protect against inflammation.

The finding that there were no proliferation or size differences in tumors from AOM–DSS-treated Apc$^{mNLS/mNLS}$ mice relative to those from Apc$^{+/+}$ mice may appear contradictory to our previous report of increased proliferation in colonic crypts from Apc$^{mNLS/mNLS}$ mice compared with Apc$^{+/+}$ mice. However, a likely explanation for this difference is that proliferation in tumors from AOM–DSS-treated mice is driven by mutations in *Ctnn1b* (b-catenin) thus over-riding any proliferation differences seen in the original tissue. These results also suggest that the role of nuclear Apc in protecting against colitis-induced tumorigenesis is at the initiation stage.

The mechanism by which APC mutations can induce inflammation is not completely known. Reduced intestinal epithelial barrier function, recently observed at an early stage of intestinal tumorigenesis driven by *Apc* mutations, would be expected to give microbial products access to the stroma, thus inducing an inflammatory response (34). The *Apc*-mutant KAD rat, which has a germline mutation resulting in truncation of the Apc C-terminus, displays a disruption of vascular endothelial cells and aberrant distribution of the junctional protein Dlg5. These rats also showed delayed colon tissue repair after induction of acute inflammation by DSS (39). The DSS-treated Apc$^{mNLS/mNLS}$ mice in this study also showed evidence of delayed tissue repair. However, Apc$^{mNLS/mNLS}$ mice express full-length Apc including the C-terminus; therefore, we do not expect the same underlying mechanism for defective tissue repair in both rodent models. In addition, because tissue repair and healing are linked to tissue damage and ulceration, our data of lagging tissue repair in DSS-treated Apc$^{mNLS/mNLS}$ mice could not differentiate between a role for nuclear Apc in preventing inflammation and a role in repair. Reduction in stem cell population and the absence of association between ulceration scores and crypt branching in Apc$^{mNLS/mNLS}$ mice may represent the severity of DSS-induced ulceration in these mice rather than a compromised ability to repair the damage. Another proposed mechanism by which mutation of *APC* compromises intestinal epithelial barrier functions is by affecting mucin production and goblet cells. Mice with an inducible *Apc* truncating mutation in their distal ileum and colon have increased barrier permeability and defective mucin production (31). A different mouse model expressing only a short Apc also showed more bacterial invasion in intestinal polyps, where both Apc

alleles are typically mutated (34). In this study, we found fewer goblet cells and a significant reduction in *Muc2* expression in DSS-treated $Apc^{mNLS/mNLS}$ mice relative to treated $Apc^{+/+}$ mice. DSS treatment has previously been associated with loss of goblet cells in general (6). However, we found that even untreated $Apc^{mNLS/mNLS}$ mice had fewer goblet cells in their small intestines and reduced *Muc2* expression in their colons compared with untreated $Apc^{+/+}$ mice (Figure 4F and G). Collectively, these data suggest that $Apc^{mNLS/mNLS}$ mice have defective mucin production, resulting in exaggerated DSS-induced inflammation and colitis-associated tumorigenicity.

Nuclear APC can repress Wnt target gene expression both *in vivo* and in cultured cells (10,13,15,40). Loss of nuclear Apc increases Wnt signaling and cellular proliferation in $Apc^{mNLS/mNLS}$ intestinal epithelial cells (19). Increased Wnt signaling by Apc mutation in other mouse models correlates with increased cellular proliferation and reduced differentiation to certain lineages, including goblet cells (30). Considering these findings, higher Wnt target expression might contribute to the increased DSS-induced inflammation and colitis-associated tumorigenicity by reducing differentiated goblet cells. One possible mechanism by which Wnt signaling controls intestinal mucus formation is by regulating the transcriptional factor Hath1, a key regulator of mucin production in colon cells. *Hath1* is negatively regulated by Wnt signaling and is reduced in CRC. Inhibition of Wnt signaling or expression of *Hath1* results in increased *Muc2* mRNA level in colon cells (41). Notably, we previously showed that untreated $Apc^{mNLS/mNLS}$ mice have reduced *Hath1* expression in intestinal epithelia (19). Together with previous reports, these data suggest that the reduction in goblet cell number in $Apc^{mNLS/mNLS}$ mice could be attributed to a reduction in goblet cell formation. However, our data could not exclude the possibility of a higher rate of goblet cell death.

Inflammation and Wnt signal upregulation are not completely independent factors. Inflammation can activate Wnt signaling through many pathways including NF-κB (1). *APC* mutations can alter retinoic acid metabolism, leading to Wnt-independent upregulation of *Cox-2*. The induced Cox-2 increases prostaglandin E2 synthesis, which in turn, activates Wnt signaling (42,43). On the other hand, Wnt signaling can increase inflammation through upregulation of inflammatory mediators such as nitric oxide synthase-2 (44) and Cox-2 (37). Cox-2 is involved in colorectal tumor formation and often upregulated in colon cancer (43). Cox-2 inhibitors have shown some therapeutic benefits in CRC (2,45). Besides being the rate-limiting enzyme in the synthesis of inflammatory mediators, Cox-2 also induces the anti-apoptotic Bcl2 (46), the angiogenic vascular endothelial growth factor (47) and the pro-tumor cytokine, IL-23 and inhibits the tumor suppressor cytokine IL-12 (48).

In conclusion, we provide evidence that nuclear Apc contributes to suppression of colitis and colitis-associated CRC. Our data support a model whereby goblet cell alterations in $Apc^{mNLS/mNLS}$ mice increases inflammation susceptibility and tumorigenicity.

Supplementary material

Supplementary Methods can be found at http://carcin.oxfordjournals.org/

Funding

National Cancer Institute (RO1 CA109220); National Center for Research Resources (P20 RR016475); National Institute of General Medical Sciences (P20 GM103418).

Acknowledgements

We thank Dr Jo Wick, Department of Biostatistics at the University of Kansas Medical Center for performing the statistical analysis of goblet cells in small intestines from untreated mice; William McGuinness for technical support with polyp assessment; Dr Jerrold Ward, Global Vet Pathology and former lab members Yang Wang and Erick Spears for critical reading of the manuscript.

Conflict of Interest Statement: None declared.

References

1. Terzić,J. *et al.* (2010) Inflammation and colon cancer. *Gastroenterology*, **138**, 2101–2114.e5.
2. Din,F.V. *et al.* (2010) Effect of aspirin and NSAIDs on risk and survival from colorectal cancer. *Gut*, **59**, 1670–1679.
3. Rowland,K.J. *et al.* (2013) The role of growth factors in intestinal regeneration and repair in necrotizing enterocolitis. *Semin. Pediatr. Surg.*, **22**, 101–111.
4. Borrello,M.G. *et al.* (2008) Inflammation and cancer: the oncogene-driven connection. *Cancer Lett.*, **267**, 262–270.
5. Camilleri,M. *et al.* (2012) Intestinal barrier function in health and gastrointestinal disease. *Neurogastroenterol. Motil.*, **24**, 503–512.
6. Pastorelli,L. *et al.* (2013) Central role of the gut epithelial barrier in the pathogenesis of chronic intestinal inflammation: lessons learned from animal models and human genetics. *Front. Immunol.*, **4**, 280.
7. Dorofeyev,A.E. *et al.* (2013) Mucosal barrier in ulcerative colitis and Crohn's disease. *Gastroenterol. Res. Pract.*, **2013**, 431231.
8. Heazlewood,C.K. *et al.* (2008) Aberrant mucin assembly in mice causes endoplasmic reticulum stress and spontaneous inflammation resembling ulcerative colitis. *PLoS Med.*, **5**, e54.
9. Ricci-Vitiani,L. *et al.* (2009) Colon cancer stem cells. *J. Mol. Med. (Berl).*, **87**, 1097–1104.
10. Neufeld,K.L. *et al.* (1997) Nuclear and cytoplasmic localizations of the adenomatous polyposis coli protein. *Proc. Natl Acad. Sci. USA*, **94**, 3034–3039.
11. Polakis,P. (2000) Wnt signaling and cancer. *Genes Dev.*, **14**, 1837–1851.
12. Neufeld,K.L. (2009) Nuclear APC. *Adv. Exp. Med. Biol.*, **656**, 13–29.
13. Rosin-Arbesfeld,R. *et al.* (2000) The APC tumour suppressor has a nuclear export function. *Nature*, **406**, 1009–1012.
14. Anderson,C.B. *et al.* (2002) Subcellular distribution of Wnt pathway proteins in normal and neoplastic colon. *Proc. Natl Acad. Sci. USA*, **99**, 8683–8688.
15. Henderson,B.R. (2000) Nuclear-cytoplasmic shuttling of APC regulates beta-catenin subcellular localization and turnover. *Nat. Cell Biol.*, **2**, 653–660.
16. Wang,Y. *et al.* (2008) Interaction between tumor suppressor adenomatous polyposis coli and topoisomerase IIalpha: implication for the G2/M transition. *Mol. Biol. Cell*, **19**, 4076–4085.
17. Jaiswal,A.S. *et al.* (2008) A novel function of adenomatous polyposis coli (APC) in regulating DNA repair. *Cancer Lett.*, **271**, 272–280.
18. Qian,J. *et al.* (2008) The APC tumor suppressor inhibits DNA replication by directly binding to DNA via its carboxyl terminus. *Gastroenterology*, **135**, 152–162.
19. Zeineldin,M. *et al.* (2012) A knock-in mouse model reveals roles for nuclear Apc in cell proliferation, Wnt signal inhibition and tumor suppression. *Oncogene*, **31**, 2423–2437.
20. Takahashi,M. *et al.* (2004) Gene mutations and altered gene expression in azoxymethane-induced colon carcinogenesis in rodents. *Cancer Sci.*, **95**, 475–480.
21. Zeineldin,M. *et al.* (2013) Understanding phenotypic variation in rodent models with germline Apc mutations. *Cancer Res.*, **73**, 2389–2399.
22. Zeineldin,M. *et al.* (2013) More than two decades of Apc modeling in rodents. *Biochim. Biophys. Acta*, **1836**, 80–89.
23. Takahashi,M. *et al.* (2000) Frequent mutations of the beta-catenin gene in mouse colon tumors induced by azoxymethane. *Carcinogenesis*, **21**, 1117–1120.
24. Cooper,H.S. *et al.* (1993) Clinicopathologic study of dextran sulfate sodium experimental murine colitis. *Lab. Invest.*, **69**, 238–249.
25. Zeineldin,M. *et al.* (2012) Isolation of epithelial cells from mouse gastrointestinal tract for Western blot or RNA analysis solation of epithelial cells from mouse gastrointestinal tract for Western blot or RNA analysis. http://www.bio-protocol.org/wenzhang.aspx?id=292#U6MfEI1dWzsce. (7 May 2014, date last accessed).
26. Cooper,H.S. *et al.* (2000) Dysplasia and cancer in the dextran sulfate sodium mouse colitis model. Relevance to colitis-associated neoplasia in the human: a study of histopathology, B-catenin and p53 expression and the role of inflammation. *Carcinogenesis*, **21**, 757–768.
27. Rencher,A.C. *et al.* (2012) *Methods of Multivariate Analysis.* 3rd edn. Wiley, Hoboken, NJ.
28. Tan,C.W. *et al.* (2013) Colon cryptogenesis: asymmetric budding. *PLoS One*, **8**, e78519.

29. Dekaney,C.M. *et al.* (2009) Regeneration of intestinal stem/progenitor cells following doxorubicin treatment of mice. *Am. J. Physiol. Gastrointest. Liver Physiol*., **297**, G461–G470.
30. Barker,N. *et al.* (2009) Crypt stem cells as the cells-of-origin of intestinal cancer. *Nature*, **457**, 608–611.
31. Grivennikov,S.I. *et al.* (2012) Adenoma-linked barrier defects and microbial products drive IL-23/IL-17-mediated tumour growth. *Nature*, **491**, 254–258.
32. Chen,L.C. *et al.* (2004) Alteration of gene expression in normal-appearing colon mucosa of APC(min) mice and human cancer patients. *Cancer Res*., **64**, 3694–3700.
33. Clapper,M.L. *et al.* (2007) Dextran sulfate sodium-induced colitis-associated neoplasia: a promising model for the development of chemopreventive interventions. *Acta Pharmacol. Sin*., **28**, 1450–1459.
34. Dennis,K.L. *et al.* (2013) Adenomatous polyps are driven by microbe-instigated focal inflammation and are controlled by IL-10-producing T cells. *Cancer Res*., **73**, 5905–5913.
35. Haertel-Wiesmann,M. *et al.* (2000) Regulation of cyclooxygenase-2 and periostin by Wnt-3 in mouse mammary epithelial cells. *J. Biol. Chem*., **275**, 32046–32051.
36. Howe,L.R. *et al.* (1999) Transcriptional activation of cyclooxygenase-2 in Wnt-1-transformed mouse mammary epithelial cells. *Cancer Res*., **59**, 1572–1577.
37. Longo,K.A. *et al.* (2002) Wnt signaling protects 3T3-L1 preadipocytes from apoptosis through induction of insulin-like growth factors. *J. Biol. Chem*., **277**, 38239–38244.
38. Harris,R.E. (2009) Cyclooxygenase-2 (cox-2) blockade in the chemoprevention of cancers of the colon, breast, prostate, and lung. *Inflammopharmacology*, **17**, 55–67.
39. Yoshimi,K. *et al.* (2013) Tumor suppressor APC protein is essential in mucosal repair from colonic inflammation through angiogenesis. *Am. J. Pathol*., **182**, 1263–1274.
40. Neufeld,K.L. *et al.* (2000) Adenomatous polyposis coli protein contains two nuclear export signals and shuttles between the nucleus and cytoplasm. *Proc. Natl Acad. Sci. USA*, **97**, 12085–12090.
41. Leow,C.C. *et al.* (2005) A role for Hath1, a bHLH transcription factor, in colon adenocarcinoma. *Ann. N. Y. Acad. Sci*., **1059**, 174–183.
42. Eisinger,A.L. *et al.* (2006) The adenomatous polyposis coli tumor suppressor gene regulates expression of cyclooxygenase-2 by a mechanism that involves retinoic acid. *J. Biol. Chem*., **281**, 20474–20482.
43. Castellone,M.D. *et al.* (2005) Prostaglandin E2 promotes colon cancer cell growth through a Gs-axin-beta-catenin signaling axis. *Science*, **310**, 1504–1510.
44. Du,Q. *et al.* (2006) Regulation of human nitric oxide synthase 2 expression by Wnt beta-catenin signaling. *Cancer Res*., **66**, 7024–7031.
45. Half,E. *et al*. (2009) Colon cancer: preventive agents and the present status of chemoprevention. *Expert Opin. Pharmacother*., **10**, 211–219.
46. Tessner,T.G. *et al.* (2004) Prostaglandin E2 reduces radiation-induced epithelial apoptosis through a mechanism involving AKT activation and bax translocation. *J. Clin. Invest*., **114**, 1676–1685.
47. Jones,M.K. *et al.* (1999) Inhibition of angiogenesis by nonsteroidal anti-inflammatory drugs: insight into mechanisms and implications for cancer growth and ulcer healing. *Nat. Med*., **5**, 1418–1423.
48. Khayrullina,T. *et al.* (2008) *In vitro* differentiation of dendritic cells in the presence of prostaglandin E2 alters the IL-12/IL-23 balance and promotes differentiation of Th17 cells. *J. Immunol*., **181**, 721–735.

Received December 5, 2013; revised May 9, 2014; accepted May 24, 2014